

Artikel 1_3

by Ariswan Ariswan

Submission date: 29-Apr-2019 09:08PM (UTC+0700)

Submission ID: 1121335167

File name: Artikel_1_3.pdf (748.26K)

Word count: 4002

Character count: 18810



26 Physicochemical Properties of Chromium-doped Titanium Dioxide Mesoporous and Its Application for Antifogging Materials

Hari Sutrisno* [a], Ariswan [b] and Dyah Purwaningsih [a]

[a] Department of Chemistry Education, Faculty of Mathematics and Natural Science, Yogyakarta State University, Kampus Karangmalang, Jl. Colombo No. 1, Yogyakarta, 55281, Indonesia.

[b] Department of Physic Education, Faculty of Mathematics and Natural Science, Yogyakarta State University, Kampus Karangmalang, Jl. Colombo No. 1, Yogyakarta, 55281, Indonesia.

*Author for correspondence; e-mail: sutrisnohari@uny.ac.id

49
Received: 28 September 2016
Accepted: 8 February 2017

ABSTRACT

Mesoporous materials of chromium doped titanium dioxide (Cr-doped TiO₂) and undoped TiO₂ were prepared by hot-injection reflux technique at 150 °C for 6 hours. Samples Cr-doped TiO₂ at different percentages: 1.1, 3.9 and 4.4 (wt% Cr) and undoped TiO₂ were synthesized from Ti(O₂)O₂·2H₂O as titanium source obtained from the reaction of TiCl₄ and H₂O₂. Solid (NH₄)₂CrO₄ was a source of chromium as dopant. The prepared materials were characterized using powder X-ray diffraction (PXRD), scanning electron microscopy-energy dispersive X-ray spectroscopy (SEM-EDS) and N₂ adsorption-desorption isotherm. The XRD results reveal that the undoped TiO₂ is composed of well-crystalline anatase (major), rutile (minor) and brookite (minor) phases. In the 1.1 wt% Cr-doped TiO₂, its phase composition is anatase (major) and rutile (minor). The chromium dioxide (CrO₂), anatase (major), brookite and silankite (TiO₂-II) are present in the 3.9 wt% Cr-doped TiO₂ and the 4.4 wt% Cr-doped TiO₂. All prepared materials (Cr-doped TiO₂ and undoped TiO₂) exhibit mesoporous of type-IV isotherm curves with H2-type hysteresis loop according to the IUPAC classification. The Brunauer-Emmett-Teller (BET) specific surface area (S_{BET}) and the mean pore size of the 4.4 wt% Cr-doped TiO₂ exhibit a maximum surface area of 111 m²/g, corresponding to mean porous size of 4.95 nm. The hydrophilic properties of Cr-doped TiO₂ were investigated with illumination of UV light. All prepared samples shows excellent superhydrophilic properties. The 4.4 wt% Cr-doped TiO₂ demonstrates the most excellent superhydrophilic properties as compared with the other samples. These results allow the materials to be prospective application as antifogging.

Keywords: titanium dioxide, Cr-doped TiO₂, mesoporous, superhydrophilic, antifogging

1. INTRODUCTION

Among the various semiconductors, titanium dioxide (TiO_2) has been well known as an efficient photocatalyst. This is because TiO_2 has the most efficient photoactivity, high refractive index, light absorption, non-toxicity, high chemical stability and relatively low-cost production [1]. When irradiated with ultraviolet or sun light on a TiO_2 surface, two phenomena of photochemical reaction will happen: the first is the photo-induced redox reactions, and the other is the photo-induced super-hydrophilic conversion. When the surface of TiO_2 was irradiated with light consisting of wavelengths shorter than its band gap, about 3.0-3.2 eV, electron and hole pairs are generated in the TiO_2 , and they reduce and oxidize adsorbates on the surface, generating radical species such as $\cdot\text{O}_2$ and $\cdot\text{OH}$. Super-hydrophilic surfaces and reduction reactions at the surface of TiO_2 are a broad research field covering such as water cleaning [2], photo-electrochemical splitting of water [3], solar cells [4], self-cleaning [5], antifogging [6], anti-bacterial surface coatings [7], and photocatalyst [8]. Various applications of self-cleaning TiO_2 films have been proposed especially for practical applications such as window glasses, mirrors and windshields of automobile [9].

The performances and the properties of TiO_2 are strongly influenced by crystalline structure, morphology, surface states, size pore, dopant and size of the particles phase [10,11]. For TiO_2 photoinduced super-hydrophilicity, the main efforts have been made in two aspects: one is to narrow the wide bandgap to extend the spectral response of TiO_2 to the visible region for the efficient utilization of the energy from the sun. Another is to reduce the recombination rate of photogenerated electron-hole pairs to enhance efficiency of photolysis. Many efforts have been made to achieve the utilization of

visible light for TiO_2 material, such as transitional metal ion doping [12, 13, 14], non-metal element doping [15, 16] and dye sensitization [17].

In the present study, a series various %wt Cr-doped TiO_2 and undoped TiO_2 have been successfully synthesized using a hot-injection reflux technique. The major goal were to synthesize and characterize undoped TiO_2 and a series various %wt chromium-doped TiO_2 and to investigate its photoinduced super-hydrophilic properties for antifogging materials.

2. MATERIALS AND METHODS

2.1 Materials

Ammonium hydroxide (NH_4OH , 28-30% NH_3) solution, hydrogen peroxide solution (H_2O_2 , 10 wt% in H_2O), ammonium chromate ($(\text{NH}_4)_2\text{CrO}_4$, 99%), titanium (IV) chloride (TiCl_4 , 99%) were purchased from Sigma-Aldrich. All the reagents were used without further purification. Titanium dioxide hydrate was obtained from the reaction of TiCl_4 and H_2O_2 [18]. In a particular procedure, 15 ml TiCl_4 was added into a 500 ml glass flask loaded in an icewaterbath, then 30 ml of H_2O_2 was added slowly into the reaction vessel under magnetic stirring. The precipitate was filtered, washed with distilled water and dried at 100 °C for 5 hours.

2.2 Sample Preparation

A series of chromium doped TiO_2 at various %wt Cr were prepared by a reflux technique. In a particular procedure, 10 g of titanium dioxide hydrate was dissolved in 50 ml of distilled water under vigorous stirring and was stirred for 4 hours to obtain colloid labeled P. For studying the effect of the $(\text{NH}_4)_2\text{CrO}_4$ concentration, in a separated beaker 0, 3, 6 and 9 wt% Cr-doped TiO_2 respectively were adopted. It was

dissolved in 20 mL of distilled water thoroughly under vigorous stirring to obtain solutions labeled Q₁, Q₂, Q₃, and Q₄ respectively. Each solution Q₁, Q₂, Q₃, and Q₄ was then slowly added to each solution P. The solution mixture was heated at 150 °C with a magnetic stirrer in equipment reflux, added dropwise NH₄OH until pH to about 8-10 within about 10 minutes. The solution mixture was refluxed at 150 °C for 6 hours. The precipitate was filtered, washed with distilled water and dried at 70 °C for 3 hours. Furthermore, the precipitate was calcined at 600 °C for 2 hours.

2.3 Physical Measurements of Samples

The morphologies of the prepared materials were observed by a scanning electron microscope (Phenom ProX Desktop SEM) equipped energy dispersive X-ray spectroscopy (EDS). Sample surface was observed and the images were recorded. EDS was used to analyze the presence of Ti, and O elements in the TiO₂ and the presence of Ti, Cr, and O elements in the Cr-doped TiO₂.

The powder XRD patterns of prepared materials were collected using a Rigaku Miniflex 600-Benchtop X-ray diffractometer, operating in the Bragg configuration using Cu K α radiation ($\lambda = 1.5406 \text{ \AA}$) at a tube current of 15 mA and a voltage of 40 kV. Data were collected over 2θ values from 2- 90°. The measurements were recorded in steps of 0.02° with a count time of 5 s/step at room temperature 25 °C. The qualitative analysis was carried out with the identification of a phase or phases in the samples by comparison with “standard” patterns: COD and ICDD. The average crystallite size of anatase and rutile were calculated based on XRD peak broadening using the basic Scherrer formula (Eq. (1)) [19], which is then modified and written as Eq. (2). It is modified

by making logarithm on both sides:

$$\beta = \frac{K\lambda}{L\cos\theta} = \frac{K\lambda}{L} - \frac{1}{\cos\theta} \quad \dots (1)$$

$$\ln\beta = \ln \frac{K\lambda}{L\cos\theta} = \ln \frac{K\lambda}{L} + \ln \frac{1}{\cos\theta} \quad \dots (2)$$

where L is the average crystallite size, β is the peak width of the diffraction peak profile at half maximum height (FWHM) resulting from small crystallite size in radians and K is a constant related to crystallite shape, normally taken as 0.9, λ is the wavelength of the X-ray radiation ($\lambda K_{\alpha}(\text{Cu}) = 1.5406 \text{ nm}$) and θ is the Bragg angle. If we plot the results of $\ln \beta$ against $\ln (1/\cos \theta)$, then a straight line with a slope of around one and then an intercept of about $\ln K/L$ must be obtained. The mean crystallite size of anatase particle was estimated by analysing the broadening of the (101), (004), (200), (211), and (220), reflections. While the mean crystallite size of rutile particle was estimated by analysing the broadening of the (110), (101), (111), (210), and (220), reflections. The average crystallite size of brookite and srilankite (TiO₂-II) were calculated based on XRD peak broadening using the Scherrer Formula (Eq.(1)).

Full adsorption-desorption isotherms data of nitrogen at 77 K on all prepared materials were collected at various partial pressures in a Surface Area and Pore Porosimetry Analyzer ASAP 2020 instrument from Micromeritics. Before the BET/B_{ET}H measurements, the prepared materials were degassed at 150 °C under vacuum for 4 h prior to analysis with a vacuum set point of 10 mmHg. The Brunauer-Emmett-Teller (BET) specific surface data area (S_{BET}) was determined by a multipoint BET method using the adsorption data in the relative pressure (P/P_0) of ~ 0.30 [20]. The pore size distribution was evaluated from the adsorption-desorption branch of the

18 isotherms by the procedure developed by Barrett, Joyner and Halenda (BJH) [21]. The nitrogen adsorption and desorption volume at the relative pressure (P/P_0) of ~ 0.99 was used to determine the pore volume and the average pore size.

2.4 Study of Photoinduced Superhydrophilic Properties

Ultraviolet-ray irradiated to the surface of the prepared sample by commercial 20W

black light blue fluorescent light, and the contact angle of water was measured every 2 minute.

38 3. RESULTS AND DISCUSSIONS

3.1 Scanning Electron Microscopy (SEM)

Figure 1 show typical SEM images and EDS analysis of TiO_2 and Cr-doped TiO_2 nanoparticles.

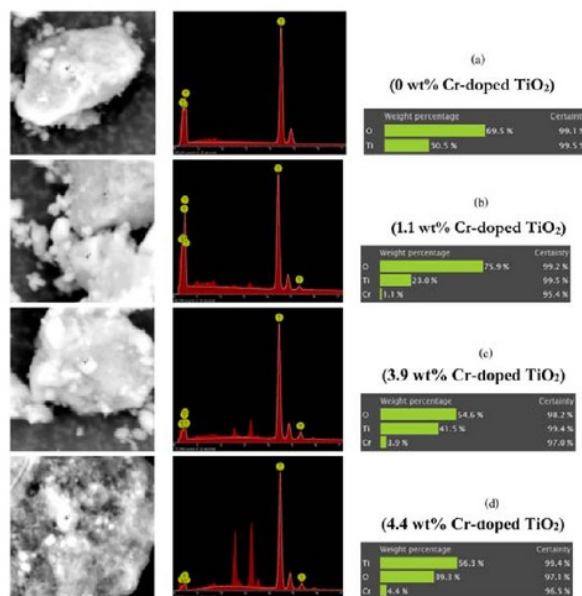


Figure 1. SEM image (left), EDS analysis (middle) and weight percentage of Ti, O and Cr in the prepared samples (right): (a) undoped TiO_2 , (b) 1.1 wt% Cr-doped TiO_2 , (c) 3.9 wt% Cr-doped TiO_2 , and (d) 4.4 wt% Cr-doped TiO_2 .

SEM micrographs and EDS spectra of TiO_2 (Figure 1(a)) and 1.1, 3.9, and 4.4 wt% Cr-doped TiO_2 (Figure 1(b-d)) prepared by reflux technique show the formation of aggregated secondary particles by the agglomeration of primary particles. On the theoretical basis, addition of each: 3, 6 and 9 wt% Cr-doped TiO_2 should produce experimentally only 1.1, 3.9 and 4.4 wt%

Cr-doped TiO_2 , respectively. The EDS analysis reveals the presence of Ti and O elements in TiO_2 and the presence of Ti, Cr and O elements in various wt% Cr-doped TiO_2 .

37 3.2 X-ray Diffraction (XRD)

Figure 2 represents the XRD patterns of undoped TiO_2 and Cr-doped TiO_2 .

The undoped TiO_2 shows that anatase (major), rutile (minor) and brookite (minor) forms are obtained by reflux technique.

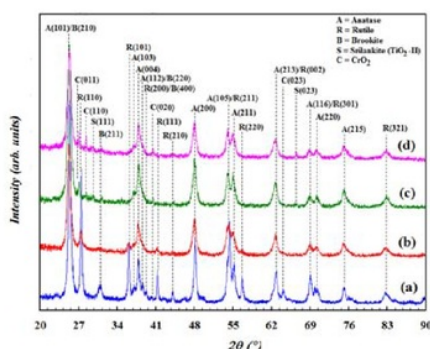


Figure 2. XRD pattern of the prepared samples: (a). undoped TiO_2 , (b). 1.1 wt% Cr-doped TiO_2 , (c). 3.9 wt% Cr-doped TiO_2 , and (d). 4.4 wt% Cr-doped TiO_2 .

From the XRD pattern (Figure 2(a)), the peak position at $2\theta = 25.36$, 37.84 , 48.11 , 54.38 , 55.07 , and 62.88 are indexed as the (101), (103), (200), (105), (211), and (213) reflections of crystalline anatase phase, corresponding to those shown in the ICDD card No. 00-021-1272. The other diffraction peaks are observed $2\theta = 27.53$, 36.14 , 39.24 , 41.32 , and 54.38 are indexed as the (110), (101), (200), (111), and (211) reflections of crystalline rutile phase, corresponding to those shown in the COD card No. 9004141. The three distinct diffraction peaks are clearly observed at $2\theta = 25.36$, 30.95 , and 39.24 being assigned to (210), (211), and (400) reflections of brookite phase, respectively, corresponding to those shown in the ICDD card No. 00-016-0617. In the 1.1 wt% Cr-doped TiO_2 , its phase composition are anatase (major) and rutile (minor). The chromium oxide (Cr_2O_3), anatase (major), brookite and srilankite ($\text{TiO}_2\text{-II}$) are present in the 3.9 wt% Cr-doped TiO_2 and the

4.4 wt% Cr-doped TiO_2 .

The phase composition, the average crystallite sizes (L) of the phases in undoped TiO_2 and Cr-doped TiO_2 are given in Table 1. It is clear that the crystallite size of anatase decreases (114.09-110.17 nm) with increasing the molar of doping agent (Cr). The crystallite size of anatase and rutile increase with the presence of doping agent (Cr).

3.3 N_2 Adsorption-Desorption Isotherm

To investigate the pore size distribution and adsorption properties of undoped TiO_2 and various wt% Cr-doped TiO_2 , N_2 adsorption-desorption isothermal tests were carried out using BET-BJH method, and their isotherm curves were presented in Figure 3. In all prepared materials, it can be observed that the powder exhibits the classical shape of type-IV isotherm curves with H2-type hysteresis loop according to the IUPAC classification [22, 23]. Their narrow hysteresis loops exhibit a typical pattern of Type IV at a relative pressure from 0.68 to 0.98 (undoped TiO_2), 0.60 to 0.92 (1.1 wt% Cr-doped TiO_2), 0.42 to 0.92 (3.3 wt% Cr-doped TiO_2) and 0.45 to 0.90 (4.4 wt% Cr-doped TiO_2), indicating that the prepared materials have characteristic of a material that contains mesoporosity and has a high energy of adsorption. In addition, the hysteresis loops for these materials are H2 which means that the material is often associated pores with narrow and wide sections and possible interconnecting channels.

The pore size distribution of undoped TiO_2 and various wt% Cr-doped TiO_2 depicted in Figure 4 (inset) show a porosity in the range of 4.95-12.16 nm. The surface area, volume and pore size distribution of the prepared materials (Cr-doped TiO_2 and undoped TiO_2) have been summarized in Table 2.

Table 1. Phase and crystallite size of undoped TiO₂ and Cr-doped TiO₂.

Sample	Phase ¹⁾	Hkl	2θ (°)	d (Å)	FWHM 2θ (deg)	L ²⁾ (nm)		
Undoped TiO ₂	Anatase	(101)	25.36	3.509	0.42	193.84		
		(004)	37.84	2.376	0.43			
		(200)	48.11	1.889	0.47			
		(211)	55.07	1.666	0.47			
		(220)	70.34	1.337	0.50			
	Rutile	(110)	27.53	3.237	0.25	323.83		
		(101)	36.14	2.483	0.29			
		(111)	41.32	2.183	0.24			
		(210)	44.13	2.050	0.26			
		(220)	56.63	1.624	0.29			
Brookite	(211)	30.95	2.887	0.67	122.99			
1.1 wt% Cr-doped TiO ₂	Anatase	(101)	25.29	3.519	0.72	114.09		
		(004)	37.75	2.381	0.74			
		(200)	48.00	1.894	0.70			
		(211)	55.12	1.665	0.49			
		(220)	70.18	1.340	0.86			
	Rutile	(110)	27.45	3.247	0.47	178.04		
		(101)	36.05	2.489	0.52			
		(111)	41.24	2.187	0.51			
		(101)	25.31	3.516	0.73			
		(004)	37.92	2.371	0.76			
3.9 wt% Cr-doped TiO ₂	Anatase	(200)	48.01	1.894	0.77	110.17		
		(211)	55.03	1.667	0.79			
		(220)	70.15	1.341	0.84			
		Brookite	(211)	31.13	2.870		0.28	294.42
		(011)	27.11	3.287	0.18			
	CrO ₂	(110)	28.40	3.139	0.10	572.86		
		(020)	40.56	2.222	0.19			
		TiO ₂ -II	(111)	29.62	3.013	0.44	186.69	
	4.4 wt% Cr-doped TiO ₂	Anatase	(101)	25.33	3.513	0.72	112.59	
			(004)	37.83	2.377	0.74		
(200)			48.01	1.894	0.76			
(211)			55.06	1.667	0.80			
(220)			70.11	1.341	0.84			
Brookite		(211)	31.29	2.8567	0.12	687.24		
		(011)	27.06	3.292	0.11			
		CrO ₂	(110)	28.39	3.141	0.20	506.69	
(020)			40.43	2.229	0.23			
TiO ₂ -II		(111)	29.53	3.022	0.39	210.58		

¹⁾ The phase composition was determined by qualitative analysis ("standard" patterns: COD and ICDD)

²⁾ The average crystallite size of anatase and rutile were calculated by Modified Debye-Scherrer formula, while for CrO₂, brookite and silankite were calculated by Debye-Scherrer formula

Table 2. Surface area, volume and pore size distribution of Cr-doped TiO₂ and undoped TiO₂ from Nitrogen Adsorption-desorption Isotherm Measurements.

Sample	Surface Area BET (S_{BET}) (m ² /g)	Pore Volume at $P/P_0 \approx 0.99$ (cm ³ /g)	Pore Size (nm)
Undoped TiO ₂	33	0.1168	12.16
1.1 wt% Cr-doped TiO ₂	65	0.1658	8.01
3.9 wt% Cr-doped TiO ₂	30	0.0591	6.88
4.4 wt% Cr-doped TiO ₂	111	0.1612	4.95

The BET surface area and the mean pore size of the 4.4 wt% Cr-doped TiO₂ exhibit a maximum surface area of 111 m²/g, corresponding to mean porous size of 4.95 nm. The pore size distribution curve calculated from the desorption branch of

the isotherm BJH analyses shows that the undoped TiO₂ exhibits pore size of 12.16 nm and the 1.1, 3.9, and 4.4 wt% Cr-doped TiO₂ exhibit pore sizes of 8.01, 6.88, and 4.95 nm (inset Figure 3), respectively.

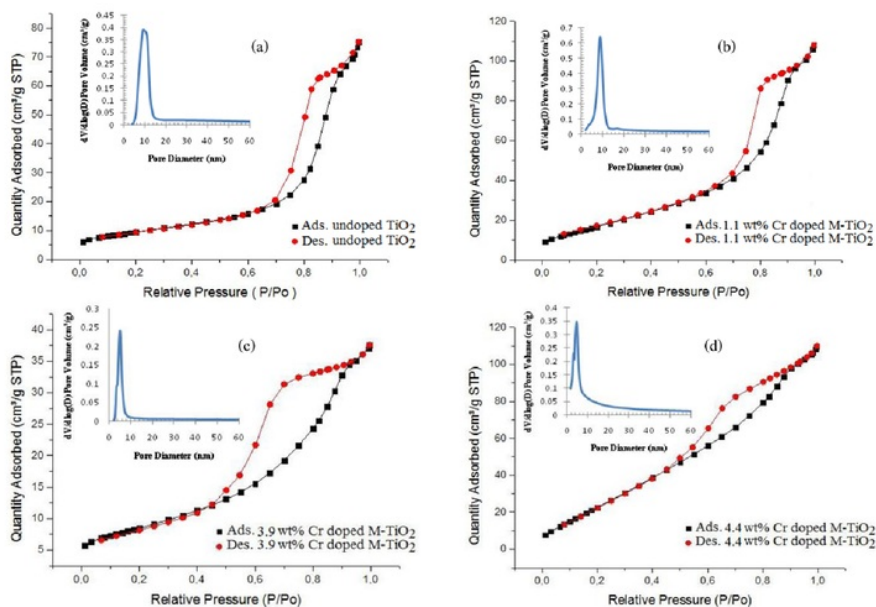


Figure 3. Nitrogen adsorption-desorption isotherms of the prepared samples: (a) undoped TiO₂, (b) 1.1 wt% Cr-doped TiO₂, (c) 3.9 wt% Cr-doped TiO₂, and (d) 4.4 wt% Cr-doped TiO₂ (inset of pore size distribution from the adsorption branch of isotherm).

3.4 The Contact Angle Changes of Water on the Cr-doped TiO₂ Surface Irradiated by Ultra-Violet (UV) Light

Figure 4 shows diagram of the change of contact angles of water dropped on the UV-irradiated undoped TiO₂ and Cr doped TiO₂ films. The contact angle of water on the prepared samples surfaces can be altered by UV irradiation.

From the diagram in Figure 4, it can be seen that the 4.4 wt% Cr-doped TiO₂ has the most excellent superhydrophilic properties as compared with other samples. The phenomena after UV irradiation for 40 minutes are as follows:

- Undoped TiO₂, irradiation with UV light inducing a decrease in contact angle from about 46.93° to 25.51°.

- 1.1 wt% Cr-doped TiO₂, irradiation with UV light inducing a decrease in contact angle from about 46.48° to 24.52°.

- 3.9 wt% Cr-doped TiO₂, irradiation with UV light inducing a decrease in contact angle from about 44.84° to 22.38°.

- 4.4 wt% Cr-doped TiO₂, irradiation with UV light inducing a decrease in contact angle from about 46.12° to 19.04°.

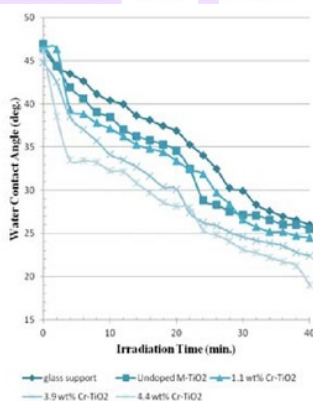


Figure 4. Change of the contact angles for film of glass support, undoped TiO₂, 1.1 wt% Cr-doped TiO₂, 3.9 wt% Cr-doped TiO₂, and 4.4 wt% Cr-doped TiO₂ with UV irradiation.

4. CONCLUSIONS

A various wt% chromium-doped TiO₂ (Cr-doped TiO₂) and undoped TiO₂ have been successfully synthesized by hot-injection reflux technique. The prepared samples consist of anatase (major), rutile (minor), chromium oxide (CrO₂) (minor), brookite (minor) and srilankite (TiO₂-II) (minor) type structures. In the 1.1 wt% Cr-doped TiO₂, its phase composition is anatase (major) and rutile (minor). The CrO₂, anatase, brookite and srilankite (TiO₂-II) are present in the 3.9 wt% Cr-doped TiO₂ and the 4.4 wt% Cr-doped TiO₂. The BET surface area and the mean pore size of the 4.4 wt% Cr-doped TiO₂ exhibit a maximum surface area of 111 m²/g, corresponding to mean porous size of 4.95 nm. All prepared materials (Cr-doped TiO₂ and undoped TiO₂) exhibit mesoporous of type-IV isotherm curves with H2-type hysteresis loop according to the IUPAC classification. The hydrophilic properties of Cr-doped TiO₂ were investigated with illumination of UV light, and all prepared samples show excellent super-hydrophilic properties, and the 4.4 wt% Cr-doped TiO₂ exhibits the most excellent superhydrophilic properties as compared with other samples. These results allow the materials to be prospective application as antifogging.

ACKNOWLEDGEMENTS

This work was financially supported by the Directorate General of Higher Education - Ministry of Education and Culture of the Republic of Indonesia based on PUPT 2014 Grant, No. 230/UPT-BOPTN/UN34.21/2014.

REFERENCES

- [1] Carp O., Huisman C.L. and Reller A., *Prog. Solid State Chem.*, 2004; **32**: 33-177. DOI10.1016/j.progsolidstchem.2004.08.001.

- [2] Dai Q., Zhang Z., He N., Li P. and Yuan C., *Mater. Sci. Eng.*, 1999; **C8-9**: 417-423. DOI 10.1016/S0928-4931(99)00016-8.
- [3] Huang C.W., Liao C.H. and Wu J.C.S., *J. Clean Energy Technol.*, 2013; **1(1)**: 1-5. DOI 10.7763/JO CET.2013.V1.1.
- [4] Dwivedi C., Dutta V., Chandiran A.K., Nazeeruddin M.K. and Gratzel M., *Energy Procedia*, 2013; **33**: 223-227. DOI 10.1016/j.egypro.2013.05.061.
- [5] Lopes de Jesus M.A.M., Trajano da Silva Neto J., Timó G., Paiva P.R.P., Dantas M.S.S. and Mello Ferreira A., *Appl. Adhes. Sci.*, 2015; **3(5)**: 2-9. DOI 10.1186/s40563-015-0034-4.
- [6] Lai Y., Tang Y., Gong J., Gong D., Chi L., Changjian Lin C. and Chen Z., *J. Mater. Chem.*, 2012; **22**: 7420-7426. DOI 10.1039/C2JM16298A.
- [7] Kong H., Song J. and Jang J., *Environ. Sci. Technol.*, 2010, **44(14)**: 5672-5676. DOI 10.1021/es1010779.
- [8] Chen F., Zou W., Qu W., and Zhang J., *Catal. Commun.*, 2009; **10**: 1510-1513. DOI 10.1016/j.catcom.2009.04.005.
- [9] Worasukhkhung S., Pudwat S., Eiamchai P., Horprathum M., Dumrongrattana S. and Aiempnanakit K., *Proc. Eng.*, 2012; **32**: 780-786. DOI 10.1016/j.proeng.2012.02.012.
- [10] Masuda Y. and Kato K., *Chem. Mater.*, 2008; **20**: 1057-1063. DOI 10.1021/cm071026t.
- [11] Testino A., Bellobono I.R., Buscaglia V., Canevali C., D'Arienzo M., Polizzi S., Scotti R. and Morazzoni F., *J. Am. Chem. Soc.*, 2007; **129(12)**: 3564-3575. DOI 10.1021/ja067050+.
- [12] Li Z., Ding D. and Ning C., *Nanoscale Res. Lett.*, 2013; **8(25)**: 1-8. DOI 10.1186/1556-276X-8-25.
- [13] Tian B., Li C. and Zhang J., *Chem. Eng. J.*, 2012; **191**: 402-409. DOI 10.1016/j.cej.2012.03.038.
- [14] Thuy N.M., Van D.Q. and Hai L.T.H., *Nanomater. Nanotechnol.*, 2012; **2(14)**: 1-8. <http://hrcak.srce.hr/file/210797>.
- [15] Nishikiori H., Hayashibe M. and Fujii T., *Catalysts*, 2013; **3**: 363-377. DOI 10.3390/catal3020363.
- [16] Yang G., Jiang Z., Shi H., Xiao T. and Yan Z., *J. Mater. Chem.*, 2010; **20**: 5301-5309. DOI 10.1039/C0JM00376J.
- [17] Gratzel M., *Inorg. Chem.*, 2005; **44**: 6841-6851. DOI 10.1021/ic0508371
- [18] Rich R.L., *Inorganic Reactions in Water*, Springer, 2006.
- [19] Monshi A., Foroughi M.R., and Monshi M.R., *World J. Nano Sci. Eng.*, 2012; **2**: 154-160. DOI 10.4236/wjnse.2012.23020.
- [20] Brunauer S., Emmett P.H. and Teller E., *J. Am. Chem. Soc.*, 1938; **60(2)**: 309-319. DOI 10.1021/ja01269a023.
- [21] Barrett E.P., Joyner L.G. and Halenda P.P., *J. Am. Chem. Soc.*, 1951; **3(1)**: 373-380. DOI 10.1021/ja01145a126.
- [22] Lowell S., Shields J.E., Thomas M.A. and Thommes M., *Characterization of Porous Solids and Powders: Surface Area, Pore Size and Density*, Springer, 2006,
- [23] Condon J.B., *Surface Area and Porosity Determinations by Physisorption Measurements and Theory*, Elsevier, 2006.

Artikel 1_3

ORIGINALITY REPORT

32%

SIMILARITY INDEX

22%

INTERNET SOURCES

22%

PUBLICATIONS

9%

STUDENT PAPERS

PRIMARY SOURCES

1	uad.portalgaruda.org Internet Source	2%
2	www.scirp.org Internet Source	2%
3	sincaf-icmse.es Internet Source	1%
4	Submitted to Prince of Songkla University Student Paper	1%
5	Dong Ri Zhang, Hai Lan Liu, Shun Yu Han, Wen Xiang Piao. "Synthesis of Sc and V-doped TiO ₂ nanoparticles and photodegradation of rhodamine-B", Journal of Industrial and Engineering Chemistry, 2013 Publication	1%
6	es.scribd.com Internet Source	1%
7	Ren, W.. "Low temperature preparation and visible light photocatalytic activity of mesoporous carbon-doped crystalline TiO ₂ ",	1%

8	Submitted to University of Bath Student Paper	1%
9	vdocuments.site Internet Source	1%
10	onlinelibrary.wiley.com Internet Source	1%
11	Chien-Cheng Tsai, Hsisheng Teng. "Chromium-doped titanium dioxide thin-film photoanodes in visible-light-induced water cleavage", Applied Surface Science, 2008 Publication	1%
12	docslide.us Internet Source	1%
13	pubs.acs.org Internet Source	1%
14	Tong-xu Liu, Fang-bai Li, Xiang-zhong Li. "TiO ₂ hydrosols with high activity for photocatalytic degradation of formaldehyde in a gaseous phase", Journal of Hazardous Materials, 2008 Publication	1%
15	Yu, H.. "Synthesis, characterization and photocatalytic activity of mesoporous titania	1%

nanorod/titanate nanotube composites",
Journal of Hazardous Materials, 20070817

Publication

16

Shrikant P. Takle, Onkar A. Apine, Jalindar D. Ambekar, Sukeshani L. Landge et al. " Solar-light-active mesoporous Cr–TiO for photodegradation of spent wash: an in-depth study using QTOF LC-MS ", RSC Advances, 2019

Publication

17

www.omicsonline.org

Internet Source

18

www.beilstein-journals.org

Internet Source

19

Feng Chen, Weiwei Zou, Wenwu Qu, Jinlong Zhang. "Photocatalytic performance of a visible light TiO₂ photocatalyst prepared by a surface chemical modification process", Catalysis Communications, 2009

Publication

20

Liu, T.x.. "TiO₂ hydrosols with high activity for photocatalytic degradation of formaldehyde in a gaseous phase", Journal of Hazardous Materials, 20080321

Publication

21

Xiaobo Chen, Shaohua Shen, Liejin Guo, Samuel S. Mao. "Semiconductor-based

1%

1%

1%

1%

1%

1%

Photocatalytic Hydrogen Generation", Chemical Reviews, 2010

Publication

22

bioresources.cnr.ncsu.edu

Internet Source

1%

23

or.nsf.gov.cn

Internet Source

1%

24

Submitted to Nanyang Technological University, Singapore

Student Paper

<1%

25

Zhao, L.. "Controlled synthesis of highly dispersed TiO₂ nanoparticles using SBA-15 as hard template", Journal of Colloid And Interface Science, 20061201

Publication

<1%

26

pendidikan-fisika.fmipa.uny.ac.id

Internet Source

<1%

27

Kapilashrami, Mukes, Yanfeng Zhang, Yi-Sheng Liu, Anders Hagfeldt, and Jinghua Guo. "Probing the Optical Property and Electronic Structure of TiO₂ Nanomaterials for Renewable Energy Applications", Chemical Reviews

Publication

<1%

28

S.A. Hassanzadeh-Tabrizi, E. Taheri-Nassaj. "Synthesis of high surface area Al₂O₃-CeO₂

<1%

composite nanopowder via inverse co-precipitation method", Ceramics International, 2011

Publication

29

issuu.com

Internet Source

<1%

30

solacolu.chim.upb.ro

Internet Source

<1%

31

Chen, Bingfeng, Fengbo Li, Zhijun Huang, Tao Lu, Yin Yuan, and Guoqing Yuan. "Integrated Catalytic Process to Directly Convert Furfural to Levulinate Ester with High Selectivity", ChemSusChem, 2013.

Publication

<1%

32

V. A. Mu'izayanti, H. Sutrisno. "Structural and optical properties of AgCl-sensitized TiO₂ (TiO₂ @AgCl) prepared by a reflux technique under alkaline condition", Cerâmica, 2018

Publication

<1%

33

Jian B. Yin, Xiao P. Zhao. " Enhanced Electrorheological Activity of Mesoporous Cr-Doped TiO from Activated Pore Wall and High Surface Area ", The Journal of Physical Chemistry B, 2006

Publication

<1%

34

Tao Zheng, Ze Tian, Bitao Su, Ziqiang Lei. " Facile Method To Prepare TiO Hollow Fiber

<1%

Materials via Replication of Cotton Fiber ",
Industrial & Engineering Chemistry Research,
2012

Publication

35 Azimi Pirsaraei, Seyed Reza, Hasan Asilian Mahabadi, and Ahmad Jonidi Jafari. "Airborne toluene degradation by using manganese oxide supported on a modified natural diatomite", Journal of Porous Materials, 2016.

Publication

36 Yu, J.. "Preparation of monodispersed microporous SiO₂ microspheres with high specific surface area using dodecylamine as a hydrolysis catalyst", Journal of Solid State Chemistry, 200601

Publication

37 ijogst.put.ac.ir

Internet Source

38 dspace.inha.ac.kr

Internet Source

39 www.docstoc.com

Internet Source

40 pubsdc3.acs.org

Internet Source

41 James B. Condon. "An Overview of Physisorption", Elsevier BV, 2006

42

Haibei Liu, Yongmei Wu, Jinlong Zhang. "A New Approach toward Carbon-Modified Vanadium-Doped Titanium Dioxide Photocatalysts", ACS Applied Materials & Interfaces, 2011

Publication

43

Park, K.W.. "Photo(UV)-enhanced performance of Pt-TiO₂ nanostructure electrode for methanol oxidation", Electrochemistry Communications, 200707

Publication

44

Mu-Hsuan Chan, Wei-Yu Ho, Da-Yung Wang, Fu-Hsing Lu. "Characterization of Cr-doped TiO₂ thin films prepared by cathodic arc plasma deposition", Surface and Coatings Technology, 2007

Publication

45

www.worldagroforestry.org

Internet Source

46

www.mdpi.com

Internet Source

47

repository.lib.fit.edu

Internet Source

48

edoc.ub.uni-muenchen.de

Internet Source

<1%

<1%

<1%

<1%

<1%

<1%

<1%

49

eprints.nottingham.ac.uk

Internet Source

<1%

50

Yu, J.. "Effects of hydrothermal temperature and time on the photocatalytic activity and microstructures of bimodal mesoporous TiO₂ powders", Applied Catalysis B, Environmental, 20070115

Publication

<1%

51

R.Preston Mason, I.Tong Mak, Mark W. Trumbore, Pamela E. Mason. "Antioxidant properties of calcium antagonists related to membrane biophysical interactions", The American Journal of Cardiology, 1999

Publication

<1%

52

Kiyoung Lee, Anca Mazare, Patrik Schmuki. "One-Dimensional Titanium Dioxide Nanomaterials: Nanotubes", Chemical Reviews, 2014

Publication

<1%

53

Monshi, Ahmad, Mohammad Reza Foroughi, and Mohammad Reza Monshi. "Modified Scherrer Equation to Estimate More Accurately Nano-Crystallite Size Using XRD", World Journal of Nano Science and Engineering, 2012.

Publication

<1%

Exclude quotes On

Exclude matches < 2 words

Exclude bibliography On

Artikel 1_3

GRADEMARK REPORT

FINAL GRADE

/100

GENERAL COMMENTS

Instructor

PAGE 1

PAGE 2

PAGE 3

PAGE 4

PAGE 5

PAGE 6

PAGE 7

PAGE 8

PAGE 9
